Force Transmission in Non-Uniform Fluid Flow by Controlling Vortices

Rishiraj Bose, Adrian Carleton, Soumitra Sitole, Yahya Modarres-Sadeghi, Frank C. Sup IV

***Abstract*— This paper investigates the use of imposed rotations of an underwater cylinder reversing direction at a desired frequency in order to transmit vortices in a flow and enable a new method of underwater force transmission. A hydrofoil interacts with controlled vortices, which modulates the forces on the hydrofoil. The motivation is to assist and resist users walking on an underwater treadmill in a continuous-flow aquatic therapy pool used for gait rehabilitation, utilizing buoyancy to reduce apparent limb weight and impact force while walking. Previously, we have shown this concept on a small scale with a passive double pendulum when the incoming fluid flow is highly uniform. This paper shows that force transmission is also possible in such a harsh environment (a continuous-flow aquatic therapy pool) where the incoming flow is highly non-uniform and at a much larger scale. By measuring forces acting on a downstream hydrofoil, we show that the frequency of the vortices generated upstream can be perceived by the downstream hydrofoil.**

I. Introduction

We report the ability of a relatively large-scale flow control system to be able to exert desired forces on an object placed in a non-uniform incoming flow. This control system is a part of our long-term goal to be able to impose human-gait trajectories during rehabilitation exercises in an underwater treadmill in a continuous-flow aquatic pool, a device that has already been studied as a therapeutic tool [1] [2].

It has been observed that energy extracted from unsteady fluid flow (vortices shed in the wake of a bluff body) can cause resonance in a flexible structure (a dead fish) placed in the wake of the bluff body and cause motion of the body [3]. Recently, we have shown that human-like gait motion can be imposed on a passive double pendulum placed in fluid flow by attaching a hydrofoil to its tip and controlling the rotation of a cylinder placed upstream [4]. When a fixed cylinder is placed in fluid flow, vortices are shed in its wake at a frequency that follows the Strouhal law [5]. This means that the frequency of vortex shedding increases linearly by increasing the incoming flow velocity. Therefore, the shedding frequency stays constant for a constant incoming flow velocity. If the cylinder is forced to rotate periodically, the frequency of vortex shedding can be controlled and stays constant to the frequency of the cylinder rotation [6]. If a hydrofoil is placed in the wake of such a cylinder, the motion of the hydrofoil can be controlled by changing the rotation frequency [6]. If the hydrofoil is free to oscillate in a plane, there are a range of system parameters for which the hydrofoil placed in the wake of the periodically rotating cylinder follows a figure-eight trajectory. If, then, this hydrofoil is attached to the tip of a double pendulum, the symmetry of its trajectory is broken, and instead of a figure-eight trajectory, it follows a teardrop trajectory– a trajectory similar to that observed in bipedal walking. This is what we have observed in our recent work [4] at a small-scale (centimeter size) and by conducting a series of experiments at the test section of a recirculating water tunnel and under highly controlled incoming flow conditions, where the incoming flow had a uniform profile. One of the challenges in scaling up this problem is that obtaining a uniform incoming flow profile in a water treadmill is nearly impossible. The question that we tackle here is whether we can transform fluid forces downstream of a rotating cylinder, the same way that we did in our previous small-scale and highly-controlled experiments, when the cylinder is placed in large-scale and highly non-uniform incoming fluid flow(Fig. 1).

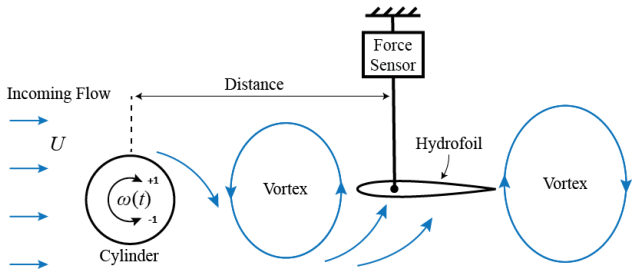

Fig. 1: Schematic of the experimental setup showing the oscillating cylinder and downstream hydrofoil with variable angle of attack.

II. Methods

We designed and built a large-scale cylinder whose rotation could be controlled externally. Fig. 2 shows the exploded view of the rotating cylinder assembly. All 3D-printed parts were made from Nylon 12 using Selective Laser Sintering (SLS) on an EOS Formiga P110 or polyethylene terephthalate glycol (PETG) using a fused deposition modeling (FDM) printer. A stationary central stainless steel shaft supported both cylinders. Each motor (Dynamixel, XW540-T140-R) was housed inside a nylon housing bolted to the gearbox enclosure. The power was transmitted through a single-stage transmission to the cylinder. The speed ratio between the actuator output and the cylinder was 1:2, meaning the gearbox was a speed multiplier. The gearbox enclosure contained the larger spur gear firmly attached to the servo motor horn. This gear meshed with the gear mounted on the outer end cap. The geared and non-geared inner end-caps

*This work was supported by the National Science Foundation through grant number CMMI-2024409.

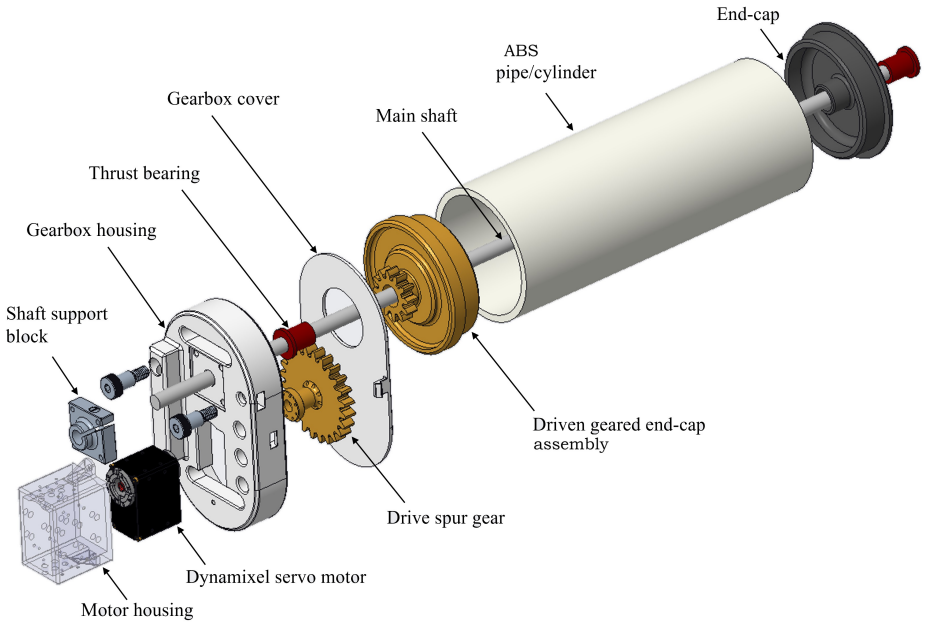

Fig. 2: Exploded view of one of the oscillating cylinder assemblies. The two cylinder assemblies share the same stationary central shaft.

are securely fastened to the 15.88cm (6.25 inch) diameter ABS cylinders using fasteners (not shown). Thrust bearings were placed inside all end-caps to reduce friction and allow smooth rotation and power transmission about the shaft. The main shaft was stationary and firmly secured to the gearbox enclosure with a stainless steel shaft support.

The entire assembly was mirrored about the distal end-cap to have two oscillating cylinders. This is done to have two actuation drives that can rotate independently and out-of-phase with respect to one another for future application of this setup of imposing walking gait trajectories wherein the hydrofoils attached to each leg of a person can be controlled independently.

The cylinder assembly was mounted via stainless-steel cross beams to the front pair of handrails. The connection was made using shoulder bolts, as shown in Fig. 2. On the handrail side, custom clamps were designed and 3D printed to mount the crossbeams to the handrails. These allowed both the height and the distance of the cylinder from the handrails to be adjusted. The motors were connected using waterproof cables to a U2D2 RS-485 to USB communication board located outside the pool, which was connected to a computer.

The cylinder was placed in the continuous-flow aquatic therapy pool with an underwater treadmill (SwimEx, 800 TWS) located at the University of Massachusetts Amherst. The dimensions of the pool are 2.38 m x 5.36 m with a maximum depth of 1.68 m. The depth of the section with the treadmill is between 1.07 - 1.37 m. Four post-holes for mounting handrails on the pool floor were used to mount the base of the rotating cylinder assembly. This allowed for mounting the components in the correct position with acceptable stability and resistance to disturbances. The entire assembly is designed to be submerged to avoid splash-backs and unnecessary alterations to the existing underwater treadmill facility.

We placed a flow straightener at the water treadmill outlet to improve the incoming flow's quality. This consisted of a 7.6 cm thick hexagonal mesh with each cell about 1 cm across. This also reduced the average incoming flow velocity, as shown in Fig. 3. The flow velocity was measured using a flow meter (Signet, 515 Rotor-X). The flow meter was connected to a plastic pipe and then sealed to protect the electronics while in the water measuring the flow. A multimeter was used to measure the frequency of the rotor. The measurements were taken in 27 approximate locations, as shown in Fig. 3. While this flow conditioning does eliminate some turbulence in the flow, its primary effect is to reduce the gradient of mean flow velocities in the vertical direction, creating a more uniform bulk flow characteristic. The flow velocity is reduced closer to the walls as expected. The experiments were carried out in the upper middle section of the flow, relatively far from the walls, where it was most consistent. As discussed in the results section, the turbulence in the flow is still sufficient to dissipate all vortices rapidly shed in the fixed cylinder case.

To quantify the forces transmitted downstream of the cylinder, we placed a hydrofoil in the wake of the cylinder at a distance of 495 mm. A pair of load cells (Omega, LC62SP) were used to measure the forces exerted on the hydrofoil in the water. The load cells were connected perpendicular to each other so that the loading direction of one was in the direction of the flow and that of the other was vertical, as shown in Fig. 4. The load cells were calibrated with

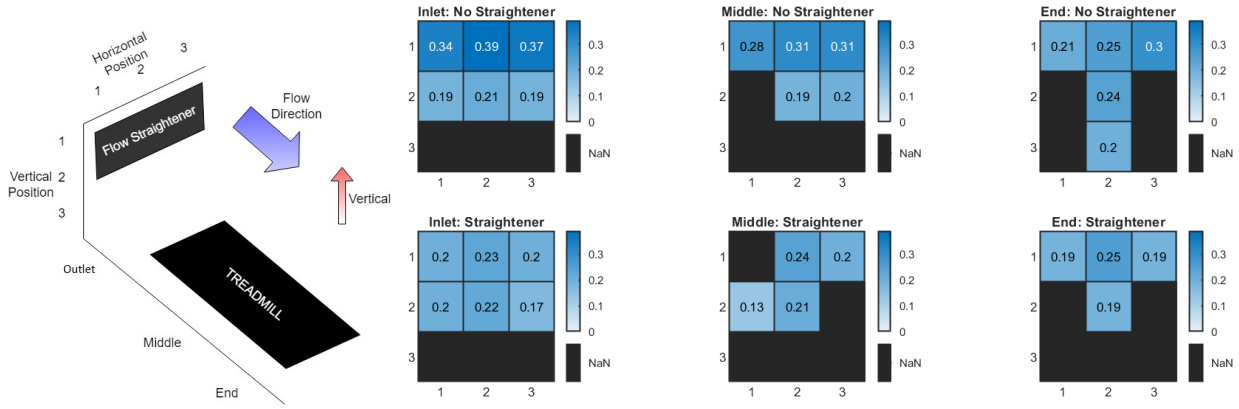

Fig. 3: Comparison of flow speeds with and without the flow straightener over cross-sections at the outlet and above the middle and end of the treadmill. All speeds are in m/s. Numbers on the grid correspond to the approximate measurement location as shown on the schematic. Note: Speeds lower than 0.1 m/s could not be measured by the instrument and are shown as a black section.

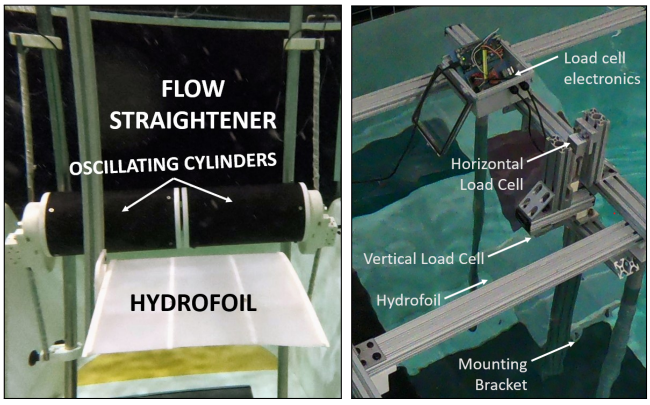

Fig. 4: Experimental setup for force measurements

standard weights using a breakout board (Avia Semiconductor, HX711), and the data recorded was streamed using a microcontroller (Arduino Due).

This assembly was mounted to an extruded aluminum frame and connected to the hydrofoil rigidly with no moving parts. The hydrofoil was a NACA 0012 [7] with a symmetric profile, with a chord length of 31.75 cm and a width of 31.75 cm. The raw force data were normalized to obtain a coefficient of drag (C_D) from the horizontal data and a coefficient of lift (C_L) from the vertical data, as these values are agnostic to the dimensions of the hydrofoil [5]:

$$C_D = \frac{2F_{horiz.}}{\rho U^2 A} \tag{1}$$

$$C_L = \frac{2F_{vert.}}{\rho U^2 A} \tag{2}$$

Both Dynamixel motors were set to the PI velocity-controlled mode to operate the cylinders. Interfacing with the motors was done using a MATLAB script using the Dynamixel API. The desired velocity profile, as determined parametrically during small-scale experiments [4], was a square wave where the cylinders changed rotation direction every half-cycle. The rotation speeds, time period of the signal, and whether the two cylinders would move in phase or out of phase were the parameters to be set at the beginning of the script. The transition between the extreme velocities was smoothed using a sinusoidal interpolation to reduce the stress on the drive train components. Five distinct signals were used to smooth the transition over 0.1s.

The incoming flow velocity was set to about 0.2 m/s, as measured by the Signet sensor. We set the ratio of the surface speed of the cylinder to the mean flow velocity, $\alpha = r\omega/U \approx 5$, and set the frequency of forcing the cylinder to rotate at 0.17 Hz. This set of parameters was previously studied by the authors of the current work [6], and places us in the range of parameters for which the shedding frequency in the wake of the cylinder is expected to be equal to the forcing frequency [8]. We set the hydrofoil at 0 degrees.

Fig. 5 shows a visualization of the flow during the shedding of a vortex from the cylinders. To achieve this, an aeration diffuser (air bubbler) was placed upstream of the cylinders and connected to a portable air compressor. The porous material of the diffuser allowed small bubbles to pass through it and into the fluid when pressurized, and these bubbles were carried by the local fluid velocity, highlighting the way the fluid moved. The bubble size can be varied by adjusting the pressure fed to the diffuser. Smaller bubbles are less buoyant and more accurately track the motion of the fluid, but if they are too small, they do not scatter enough light towards the camera to be visible. In the highly turbulent flow of the treadmill, larger bubbles were required to visualize the flow, and these were illuminated with a high-intensity LED underwater light. In Fig. 5(a), the cylinders are rotating clockwise. This causes the flow to follow the rotation of the cylinder and curve downward in the wake of the cylinders. In (b), the cylinder's rotation direction has just switched, and the fluid nearest to the cylinder is forced to curve upward, creating a region of high-velocity gradient in

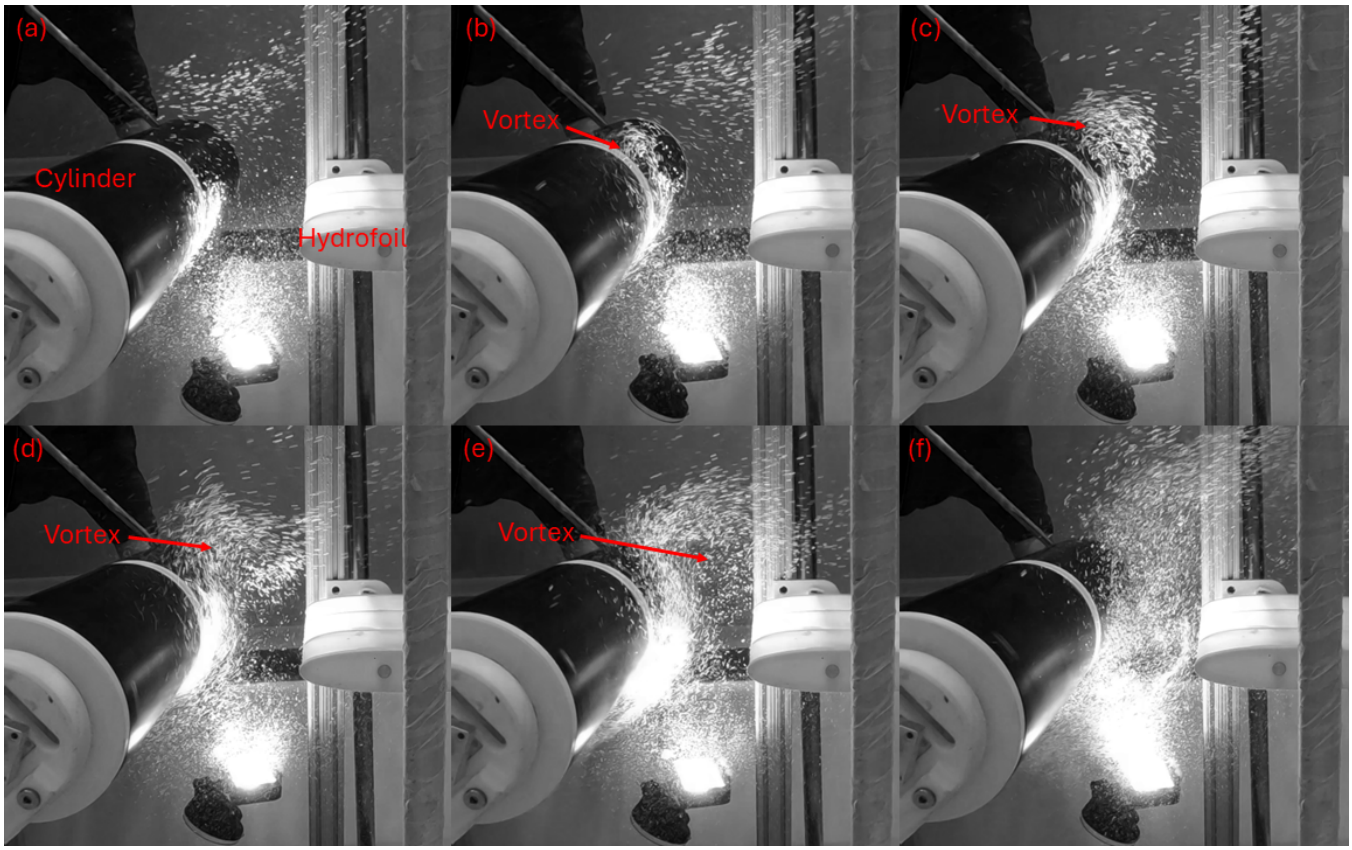

Fig. 5: Flow visualization of a vortex being shed from the cylinder. Here the flow is from left to right, and is seeded with air bubbles to show the motion of the fluid. These bubbles are illuminated by the high-intensity LED light visible at the bottom of each panel. Panels (a) and (b) are before and during vortex formation; panels (c), (d), and (e) show how the vortex separates from the cylinders, moves downstream, and interacts with the hydrofoil, and panel (f) shows the flow straightening out before the formation of the next vortex. The supplemental video shows the vortices being formed in real-time.

the wake and forming a vortex. In (c), the vortex is fully formed and begins to separate from the cylinders. In (d), the vortex is separated from the cylinder and travels downstream with the mean fluid flow before contacting and dissipating on the hydrofoil in (e). In (f), the flow is straightening out, but unlike in (a), the flow now has an upward curve as the cylinder is rotating in the counter-clockwise direction.

III. Results

The forces that are measured at the hydrofoil are shown in Fig. 6 for two cases: first, when the cylinder is not rotating (left) and then when the cylinder is periodically rotating (right). In the case of a fixed cylinder placed in uniform flow, it is expected that vortices are shed in the wake of the cylinder at a frequency predicted by the Strouhal law. In less adverse flow, we would expect these vortices to travel downstream and interact with the hydrofoil and, therefore, exert non-zero lift and drag forces on the hydrofoil. In the case shown here, however, clearly, the hydrofoil is not affected by the presence of these vortices, and the fluctuating forces that act on the hydrofoil are practically zero. This is due to the high degree of non-uniformity in the incoming flow in a water treadmill. Once the cylinder is forced to rotate (the right plots in Fig. 6), fluctuating forces are indeed measured at the hydrofoil at frequencies equal to the forcing frequency and twice that, as seen in the form of two peaks in the FFT plot in the figure. These fluctuating forces result from the vortices formed due to the rotation of the cylinder maintaining their structure long enough to travel downstream and interact with the hydrofoil. This shows that by actively controlling the vortex shedding of cylinders through periodic rotation, we can induce a much higher degree of coherence in said vortices than passive shedding can. In fact, the imposed rotation increases the synchronization of vortex generation along the length of the cylinder, resulting in a measurable fluctuating lift and drag at the hydrofoil location.

A. Time lag estimation

This temporal delay between the oscillation of the cylinders and the force spike is demonstrated in Fig. 7 (The oscillation phase is shown as per Fig. 1). If we impose a periodic rotation on the cylinder, then we can induce the vortices in its wake despite the non-uniform incoming flow because a rotating cylinder synchronizes the shedding of vortices in the wake and the effect being picked up by the hydrofoil. The length of the delay between the vortex being

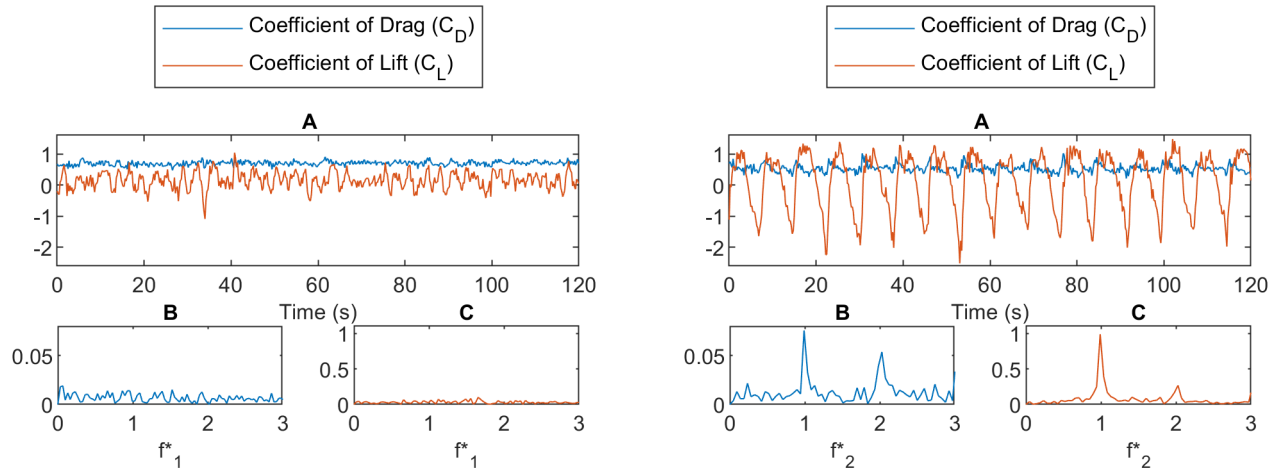

(a) Only flow turned on

(b) Flow turned on and cylinders oscillating

Fig. 6: Comparison of the forces on hydrofoil with the oscillation of the cylinders turned on and off. **A** shows the time variation of the drag coefficient and the lift coefficient. **B** and **C** show the FFTs of the drag and lift coefficients, respectively. Frequencies are normalized by the expected vortex shedding frequency as $f_1^* = f/f_s$ where f_s is the shedding frequency predicted by the Strouhal law ($St = f_s D/U$, where St is the Strouhal number, D is the characteristic length, and U is the mean flow speed) and $f_2^* = f/f_c$ where f_c is the frequency of cylinder oscillation of $0.17Hz$.

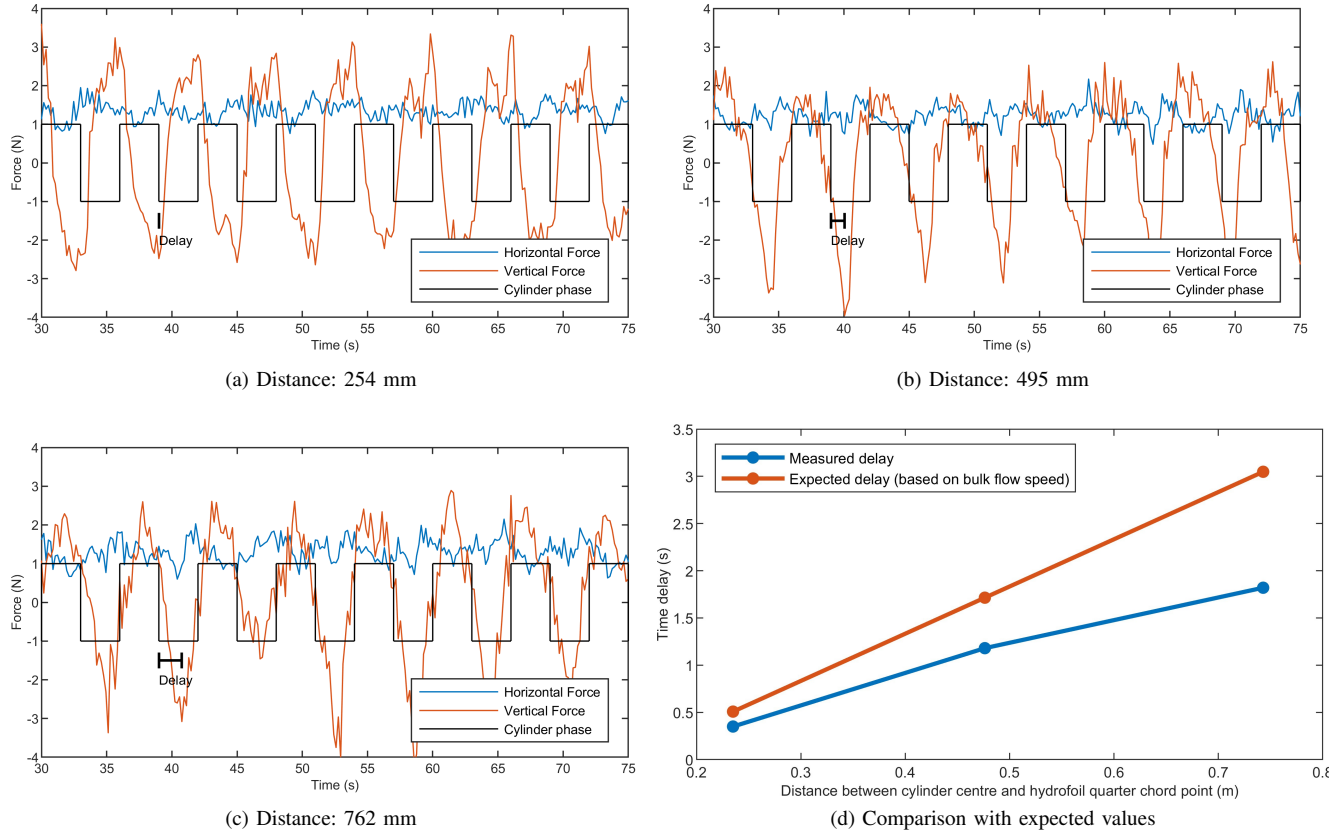

(a) Distance: 254 mm

(b) Distance: 495 mm

(c) Distance: 762 mm

(d) Comparison with expected values

Fig. 7: Time delay between the signal generated at the cylinder and the effect on the hydrofoil compared at different distances between the cylinder center and hydrofoil quarter chord point. +1 means the top of the cylinders is spinning in the flow direction, and -1 means it is spinning against it (refer to Fig. 1).

generated and its effect on the hydrofoil is influenced by the speed of the water and the distance between the hydrofoil and the cylinders. The observed delay is calculated using the vertical forces as it has more pronounced peaks. It is assumed that the force in a particular direction (either up or down) peaks right before the center of the vortex reaches the tip of the hydrofoil as the direction of flow reverses at this point. The expected values are calculated based on the bulk flow speed measured earlier and the distance between the surface of the cylinders and the tip of the hydrofoil.

IV. Conclusion

By forcing a cylinder to rotate periodically, we show that vortices can be generated at a desired frequency (forcing frequency) in its wake, even if the cylinder is placed in highly non-uniform fluid flow. The shedding of vortices in the wake of any cylinder placed in a high Reynolds number flow, fixed or forced to rotate periodically, has been observed previously in the cases of a uniform incoming flow. In the experiments that we present here, we show that these vortices are not observed in the underwater treadmill that we have used for these experiments if the cylinder is fixed (with no rotation), due to the extreme non-uniformity that is introduced to the incoming flow. If we impose a periodic rotation on the cylinder, then we can induce vortices in its wake despite the non-uniform incoming flow, because a rotating cylinder synchronizes the shedding of vortices in the wake. We quantify the presence of these vortices in the wake of a cylinder by measuring lift and drag forces on a hydrofoil placed in the wake of the cylinder.

In order to use this approach to control an object, it is necessary to characterize the system dynamics. Because of the highly turbulent flow in the water treadmill, it is not feasible to derive a deterministic model of the force transmission. Quantifiable experimental results and observed behavior are, therefore, crucial to utilizing this system for practical applications. To this end, further parametric experiments must be performed to analyze the effect of other controllable variables, such as the angle of attack of the hydrofoil and the waveform of the input signal to the cylinders.

This work is a part of our long-term project in which we intend to influence walking gait trajectories in persons using an underwater treadmill in a continuous-flow aquatic therapy pool by controlling the vortices shed in the wake of an upstream cylinder. These vortices would interact with hydrofoils that would be attached to the shanks of a person (similar to the hydrofoils that we have used in the experiments discussed here), and since they exert forces on these hydrofoils, the induced forces can guide a person's limb toward a desired motion. In this paper, we have shown the feasibility of this approach at a smaller scale with a low-impedance double pendulum before, and here we are working toward scaling up this approach and moving toward human subject testing.

ACKNOWLEDGMENT

The authors would like to thank the UMass Amherst Athletics Department and David Maclutsky and Kristen Hastings for allowing access to the underwater treadmill facility for testing. The authors would also like to thank Ali Adil Lashari for his help designing the experimental hardware and Leah Metsker for helping with data collection.

References

[1] A. M. F. Barela, S. F. Stolf, and M. Duarte, "Biomechanical characteristics of adults walking in shallow water and on land," *J. Electromyogr. Kinesiol.*, vol. 16, no. 3, pp. 250–256, Jun. 2006.

[2] L. C. Carneiro, S. M. Michaelsen, H. Roesler, A. Haupenthal, M. Hubert, and E. Mallmann, "Vertical reaction forces and kinematics of backward walking underwater," *Gait & Posture*, vol. 35, no. 2, pp. 225–230, Feb. 2012.

[3] D. N. Beal, F. S. Hover, M. S. Triantafyllou, J. C. Liao, and G. V. Lauder, "Passive propulsion in vortex wakes," *Journal of Fluid Mechanics*, vol. 549, p. 385–402, 2006.

[4] A. G. Carleton, F. C. Sup, and Y. Modarres-Sadeghi, "Passive double pendulum in the wake of a cylinder forced to rotate emulates a cyclic human walking gait," *Bioinspiration & Biomimetics*, vol. 17, no. 4, p. 045006, Jun 2022.

[5] Y. Modarres-Sadeghi, *Introduction to Fluid-Structure Interactions*. Springer Nature, Feb 2022.

[6] T. M. Currier, A. G. Carleton, and Y. Modarres-Sadeghi, "Dynamics of a hydrofoil free to oscillate in the wake of a fixed, constantly rotating or periodically rotating cylinder," *J of Fluid Mechanics*, vol. 923, p. A21, 2021.

[7] E. N. Jacobs, K. E. Ward, and R. M. Pinkerton, *The Characteristics of 78 related airfoil section from tests in the Variable-Density Wind Tunnel*. US Government Printing Office, 1933, no. 460.

[8] P. T. Tokumaru and P. E. Dimotakis, "Rotary oscillation control of a cylinder wake," *Journal of Fluid Mechanics*, vol. 224, p. 77–90, 1991.